Feedforward and Feedback Processing of Spatiotemporal Tubes for Efficient Object Localization

Khari Jarrett[1], Joachim Lohn-Jaramillo[1], Elijah Bowen[2], Laura Ray[1] and Richard Granger[2]
[1]*Thayer School of Engineering, Dartmouth College, 14 Engineering Drive, Hanover, NH, U.S.A.*
[2]*Department of Psychology and Brain Sciences, Dartmouth College, Hanover, NH, U.S.A.*

Keywords: Top-down Visual Processing, Video Tracking, Action Localization.

Abstract: We introduce a new set of mechanisms for tracking entities through videos, at substantially less expense than required by standard methods. The approach combines inexpensive initial processing of individual frames together with integration of information across long time spans (multiple frames), resulting in the recognition and tracking of spatially and temporally contiguous entities, rather than focusing on the individual pixels that comprise those entities.

1 INTRODUCTION

A human watching a video can recognize and distinguish actions taken by entities, and can track them across time. Much current research uses optic flow to capture relatively dense motion information, typically frame by frame (Grundmann *et al.*, 2010; Lee, Kim and Grauman, 2011; Jain *et al.*, 2014; Caelles *et al.*, 2016); yet to a human, the video is readily recognizable even if frames are dropped, or the time resolution is altered (changing the content of all the frames), or if motion is temporarily occluded.

We hypothesize that humans are integrating contiguous information across longer time spans than individual frames, and are using a specific set of identified regularities, that can be extracted from these longer time spans to generate expectation-based assumptions and simplifications of the actions, rendering activities independent of the information in any specific frame.

The many challenges to video processing include changing backgrounds, lighting, camera motion, occlusion, and multiple moving entities. We proffer a multi-step approach that incorporates inexpensive processing of individual frames together with further processing of frames in the context of other nearby frames. We demonstrate that this straightforward approach enables recognition and tracking across time with substantially less expense than current standard methods. The methods described here constitute a novel localization scheme that encodes motion information using less data than current state of the art systems.

To reduce the amount of data necessary to recognize motion, we consider object-level instead of pixel-level motion information. Rather than considering an optical flow vector per pixel per frame, we consider a bounding region around an object and a single vector associated with the object, not its constituent pixels. This approach drastically reduces the amount of data necessary to describe the motion in the video. Our approach has a few notable advantages as listed below:

1. Our framework is derived from both brain circuit analyses and behavioural psychophysics findings, and yet does not include artificial neural networks (ANNs), so we avoid the large associated computational costs, and the need to train on large datasets;
2. Our approach allows for the concurrent tracking and localization of multiple entities/actions;
3. Our approach uses low-data representations of individual frames, along with enhanced representations of multi-frame sequences, lending itself to rapid and inexpensive top-down recognition and localization processes.

Jarrett, K., Lohn-Jaramillo, J., Bowen, E., Ray, L. and Granger, R.
Feedforward and Feedback Processing of Spatiotemporal Tubes for Efficient Object Localization.
DOI: 10.5220/0007313603770387
In *Proceedings of the 8th International Conference on Pattern Recognition Applications and Methods (ICPRAM 2019)*, pages 377-387
ISBN: 978-989-758-351-3

2 RELATED WORK

2.1 Motion for Visual Understanding

It is understood that motion perception is pivotal to early stage pattern recognition and ultimately the human visual system (Lu and Sperling, 1995). It has been demonstrated that walking or any repetitive human movement may be recognized via bottom-up processing techniques (Polana and Nelson, 1994). Support of bottom-up techniques came from (Giese and Poggio, 2003), who demonstrated the neurophysiological plausibility of a feedforward model for visual recognition of complex movements. Furthermore, evidence suggests primates consider the form and motion of a scene separately before combining the cortical pathways (Oram and Perrett, 1996). These insights have encouraged much of the work in visual learning and action recognition (Gavrila, 1999; Poppe, 2010).

Since its introduction via the seminal paper (Horn and Schunck, 1981), optical flow remains the state-of-the-art in motion representation. Work has been done in the field to build on the optical flow approach including: optimizing the accuracy of an optical flow estimate (Roth, Lempitsky and Rother, 2009), estimating large motion in smaller structures (Brox and Malik, 2010a), and extending optical flow for long-term motion analysis (Brox and Malik, 2010b). Inspired by the success of image segmentation, (Tsai *et al.*, 2012; Galasso *et al.*, 2014; Jain and Grauman, 2014) propose performing image segmentation on each video still and linking them through time via optical flow. Others, citing its inaccuracy and/or high computational costs, opt to replace optical flow front ends with relatively cheap, hand-crafted motion vectors (Tsai, Yang and Black, 2016; Zhang *et al.*, 2016).

2.2 Motion for Object Segmentation

Researchers have demonstrated that incorporating dense motion information for object segmentation provides better results than using color information alone (Wang *et al.*, 2011; Simonyan and Zisserman, 2014). This discovery, combined with the advancement of the superpixel as a tool in image processing (Shi and Malik, 1997; Fulkerson, Vedaldi and Soatto, 2009), led to the development of “super-voxel” strategies (Tsai *et al.*, 2012). A popular approach is to use dense optical flow to oversegment video into super-voxels that are then hierarchically merged until an action is localized (Grundmann *et al.*, 2010; Jain *et al.*, 2014). Optical flow orientations are used to provide depth-independent pixel clustering (Narayana *et al.*, 2013). Another technique uses a CNN to rank how likely a potential spatiotemporal region is to contain a moving object (Tokmakov, Schmid and Alahari, 2017).

To outperform supervoxel methods, (Chang, Wei and Fisher, 2013) introduced and developed “temporal superpixel” methods. (Pathak *et al.*, 2016) propose an unsupervised motion-based approach to segment foreground objects at the pixel level, then using the resulting segmentations to train a CNN to segment from the static frames of a video.

2.3 CNNs for Action Recognition

Recent action-recognition approaches incorporate both spatial and motion features to train classifiers to distinguish different types of actions (Wang *et al.*, 2011; Simonyan and Zisserman, 2014; Zhang *et al.*, 2016). These approaches exploit the computational power of convolutional neural networks (CNNs), which generally yield strong results but require a large amount of training data and computational cost. CNNs became popular due to their success in the image classification field (Krizhevsky, Sutskever and Hinton, 2012; He *et al.*, 2015). Though critics of CNNs highlight the fact that neural networks are easily fooled into misclassification (Nguyen, Yosinski and Clune, 2014), CNNs remain pivotal to current methods being developed for action recognition. Some approaches consider spatial features and temporal features separately, using the input pixels as the spatial representation and multi-frame optical flow as the temporal representation, and combining the information at a later stage to generate a class (Simonyan and Zisserman, 2014). Other approaches use dense optical flow to sample dense trajectories from a video, which can be encoded into feature descriptors and evaluated with a bag-of-features classifier (Wang *et al.*, 2011).

2.4 Single Target Localization/Recognition

The existence and development of large video datasets such as DAVIS, UCF 101, HMDB51, or Thumos-2014 (Soomro, Zamir and Shah, 2012; Kuehne *et al.*, 2013; Jiang *et al.*, 2014; Perazzi *et al.*, 2016) has facilitated research in action recognition. However, the convention of a single target action per video has skewed progress away from the problem of recognizing multiple entities performing actions concurrently. Furthermore, it has forcefully encouraged the field toward CNNs. Most action

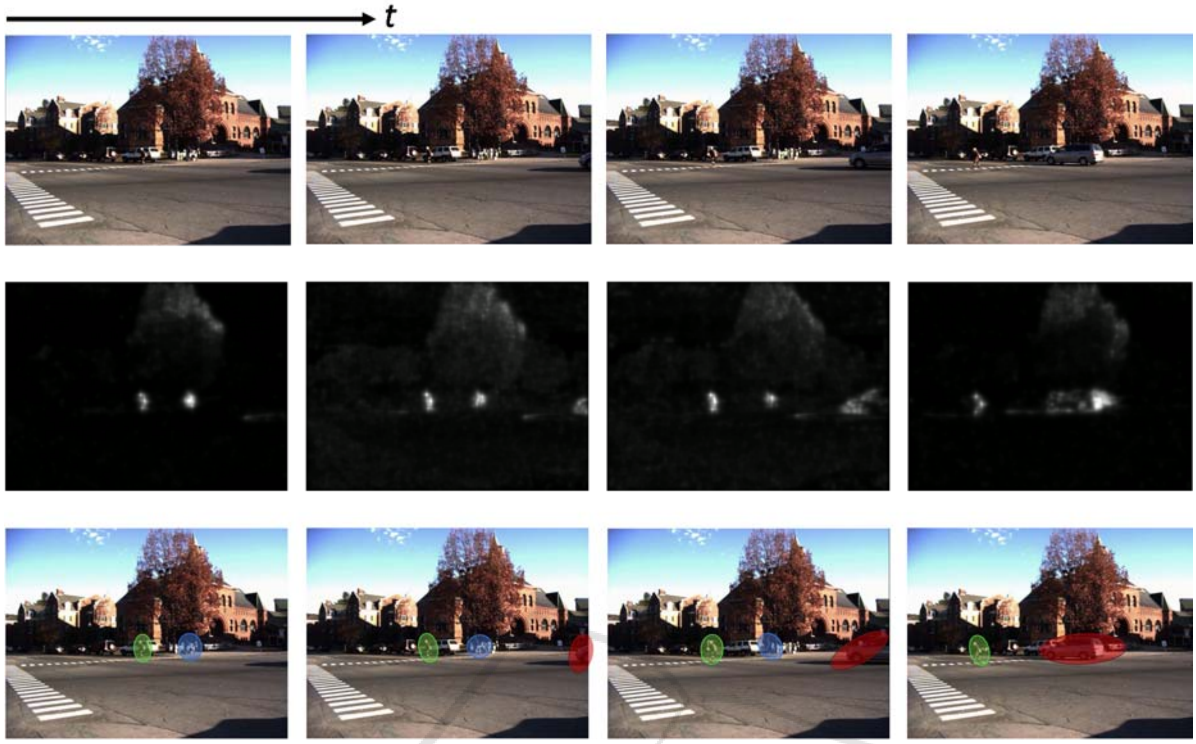

Figure 1: Subsequent frames of three separate processes. The first row is the input video. The second row is a simulated output of the magnocellular pathway in the human visual system. We use it to extract low frequency motion information. Bright pixels correspond to detected motion, while dark pixels correspond to a lack thereof. The third row is the result of our method. Note that ellipses are constructed around groups of moving pixels.

localization techniques, temporal or spatiotemporal, use CNNs to analyze video to make a single determination about how the action of interest should be isolated (Simonyan and Zisserman, 2014; Gkioxari and Malik, 2015; Tran *et al.*, 2015; Caelles *et al.*, 2016; Shou *et al.*, 2016; Zhang *et al.*, 2016). In a departure from previous work, we propose a method to handle simultaneous action localization of multiple targets. As a result, performing our method on available datasets and benchmarks limits the potential questions.

3 OVERVIEW OF APPROACH

The primary goal is to spatially and temporally localize each separate moving foreground entity in videos “from the wild.” Furthermore, we suggest a localization tool that also functions as a compact representation of each entity’s motion. We accomplish this by enclosing each moving foreground entity within a *tube*, a sequence of *ellipses* on consecutive frames as illustrated in Figure 2. Each ellipse exists on a single frame and encloses a temporal cross section of a moving entity. Each ellipse is represented by an eight-element vector of ellipse properties. For an ellipse e, the ellipse vector is

$$e = [x, y, a, b, \phi, f, Vx, Vy], \tag{1}$$

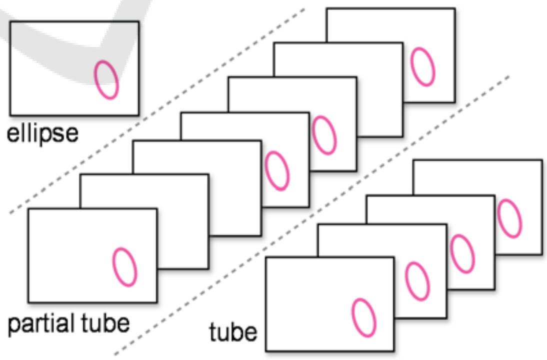

Figure 2: A visualization of an ellipse, a partial tube, and a tube. Note that the ellipse exists on a single frame and its descriptor contains the center location, size, rotation angle, frame present, and velocity. Both the partial tube and tube are lists of ellipses. A partial tube does not contain ellipses at dense frames. A tube does.

where (x, y) is the center of the ellipse and a, b, and ϕ are the semi-major axis length, semi-minor axis length, and the angle of rotation (counterclockwise from the x-axis to the major axis) respectively. Property f is the frame of the video where the ellipse is present and Vx and Vy are the Cartesian velocity components of this ellipse at frame f. The x property of ellipse e is denoted e_x.

We detail and propose a four-step process to create tubes from input video data. Given a video with T frames $\{F_t\}_{t=1\ldots T}$ we find a list of tubes such that each encompasses a foreground object. Note that none of the following methods require the use of spatial information.

3.1 Alg. 1: Magnocellular Motion Processing

At each video frame, we invoke the work of (Benoit *et al.*, 2010) to perform biologically inspired low level image processing replicating the magnocellular retino-thalamic pathway of the mammalian visual system. This method is distinct from typical "background subtraction" schemes due to the presence of a relative sensitivity and memory/time decay associated with identified motion. This naturally introduces a hierarchical attention span based on relative size, magnitude of motion, and motion duration.

Algorithm 1
Input: a test video $\{F_t\}_{t=1\ldots T}$
Output: a list of ellipses **L** = {e}
For $t = 1 \ldots T$
  M_t = Magno(F_t)
  B_t = Threshold(M_t, mean(M_t))
  For each contour $c \in B_t$
    e = FitEllipse(c)
    Add e to **L**

Algorithm 1 reads the input video and creates a list of ellipses that spatially enclose foreground moving objects.

Notably, the output of this magnocellular processing provides motion information that would be completely unavailable from individual still frames alone. The method captures motion that is abstracted from average motion spanning multiple frames. The identified pixel locations are reduced via a threshold set according to the mean pixel value in the magnocellular output. This creates a binary image with groups of "activated" pixels, which we erode then dilate.

An ellipse is then fitted around each surviving group of pixels. After filtering out ellipses with a semi-major axis less than equal to five pixels, each ellipse's identifying information is stored onto a list. The result is a list of ellipses, each of which enclose a moving object in the foreground.

3.2 Alg. 2: Constructing Partial Tubes

The list of ellipses becomes input to the creation of a sequence of ellipses, termed a *partial tube*. This is our primary attempt at locating an entity across time. First, the ellipses are gathered in groups G_t based on the frame number, f, of each. Since only one ellipse is selected per partial tube per group, the width of the bin (in frames) is a hyperparameter. A larger bin size encourages a scarcer localization of the entity across time. In the limit as bin size is decreased, Algorithm 2 approaches a frame-by-frame analysis. We chose our bin size as 5 frames (i.e., ellipses in frame 6-10 are in a group, ellipses in 11-15 are in the next group, etc.). We then pair each ellipse in a group with its "best match" in the next group.

Algorithm 2 organizes the list into paths that represent an entity's motion through time.

The best match is defined as follows. Let ellipse $e \in G_t$ and ellipse $g \in G_{t+5}$. If velocity information is available for e, we use it to create a "prediction ellipse" at the expected location of e in each frame in G_{t+5}. Then, g is the best match ellipse if and only if it is the closest of all ellipses in G_{t+5} to its prediction

Algorithm 2
Input: a list of ellipses **L** = $\{e\}$
Output: a list of partial tubes $\{\mathbf{P}_i\}_{i=1\ldots N}$
For $t=1,6,11,\ldots,T$
  $G_t = \{e \in \mathbf{L} \mid e_f \in [t, t+4]\}$
For each G_t ($G_1, G_6, G_{11}, \ldots, G_T$)
  For each ellipse $e \in G_t$
    $e' \in G_{t+5}$ = BestMatch(e, G_t, G_{t+5})
    If $e \in \{\mathbf{P}_i\}_{i=1\ldots n}$ → Add e' to $\mathbf{P}_i$
    Else → create $\mathbf{P}_{n+1}$ and add e, e' to $\mathbf{P}_i$

Function: BestMatch
Input: ellipse $e \in G_t$, group G_t, next group G_{t+5}
Output: ellipse $e' \in G_{t+5}$
If e_{Vx} is empty→ e' = closest $e \in G_{t+5}$ in size and distance
Else → **For** $s = t+5\ldots t+9$
  e^* = predict ellipse at frame s using e_{Vx}, e_{Vy}
  e' = closest in distance to e^*
$e'_{Vx} = (e'_x - e_x) / (e'_f - e_f)$
$e'_{Vy} = (e'_y - e_y) / (e'_f - e_f)$

ellipse. If the velocity information does not yet exist (i.e., the ellipse belongs to the first group in the video or is the start of a new entity), g is the best match to e if and only if it is the closest in G_{t+5} to e via size and distance.

Once an ellipse pairing occurs, two important things happen. First, since we assume the pair of ellipses are two different temporal cross sections of the same object, we can calculate the velocity (in pixels/frame) between the center of each ellipse using the forward difference method. This information is stored simply as two scalar properties, Vx and Vy, of the latter ellipse. Second, pairs of ellipses are stored as *partial tubes* unless the former ellipse of the pair already belongs to another partial tube. In that case, the latter ellipse in the pair is simply appended to the same partial tube.

We iterate through the frames of the video repeating the grouping and pairing process, to create partial tubes. Each *partial tube* is a list of ellipses that corresponds to one potential foreground object.

3.3 Alg. 3: Tube Completion

The partial tubes create a sparse localization of the potential foreground entities in the video, existing approximately once per every bin size, unlike the continuously present entities they are meant to represent. For the representation to be like the entity, *an ellipse must exist at every frame between the start and end frames of the entity*. Algorithm 3 makes tubes by defining and creating ellipses between existing ellipses in the partial tube.

We consider each partial tube separately. For every frame, t, in a partial tube, **P**, we construct a group, C, that consists of every ellipse $e \in \mathbf{P}$ "near" frame t. To be near frame t is to be within half of binsize (rounded down to nearest integer) away from t (i.e., $e_f \in [t\text{-}2, t\text{+}2]$). If nothing is near t, we extend the definition to include any ellipse within binsize of t (i.e., $e_f \in [t\text{-}5, t\text{+}5]$). The ellipses grouped in C are used to artificially smooth the properties of the ellipse at t.

At each frame, we check if an ellipse exists in the partial tube. If it does, the ellipse becomes a part of the new tube. Otherwise, we interpolate the value of the new x and y coordinates using the nearest ellipses before and after frame t. The a and b properties of our new ellipse are defined as the maximum a and b values across C. The orientation, ϕ, of the new ellipse is chosen as the ϕ of the closest ellipse in the partial tube. The velocities, Vx and Vy, are defined as the average Vx and Vy across C.

Algorithm 3

Input: a list of partial tubes $\{\mathbf{P}_i\}_{i=1\ldots N}$
Output: a list of tubes $\{\mathbf{T}_i\}_{i=1\ldots N}$
For each partial tube $\mathbf{P}_i = \{e\}$
    For each frame $t = min(e_f \in \mathbf{P}_i), \ldots, max(e_f \in \mathbf{P}_i)$
        $C = \{e \in \mathbf{P}_i \mid e_f \in [t\text{-}2, t\text{+}2]$ or $[t\text{-}5, t\text{+}5]$ (if empty)$\}$
        $e'_x, e'_y \leftarrow$ Interpolate from prev(e) to next(e)
        $e'_a, e'_b \leftarrow$ max e_a, e_b over C
        $e'_\phi = e_\phi$ of nearest $e \in \mathbf{P}_i$
        $e'_{Vx}, e'_{Vy} \leftarrow$ average e_{Vx}, e_{Vy} over C
        $e'_f = t$
        Add e' to $\mathbf{P}_i$
    $\mathbf{T}_i = \mathbf{P}_i$

Algorithm 3 interpolates between sparse ellipses in each partial tube to create a tube, the union of a sequence of ellipses across consecutive frames.

After repeating the grouping and interpolating process for each frame in the partial tube, the result is a list of ellipses at every frame. This representation, shown in Figure 3, is henceforth referred to as a ***tube.*** The process is repeated for each partial tube, resulting in a list of tubes.

3.4 Alg. 4: Tube Merging

Immediately after tube creation, a single entity, as defined by human perception, is occasionally represented by a union of several tubes instead of a single tube. Usually, this is a result of one or more occlusions. Consider the case shown in Figure 3. In the first video, the pedestrian on the left is represented by two separate tubes. By connecting those tubes across the occlusion, we keep track of the entity. Algorithm 4 connects tubes that likely cover the same entity. To that end, we must first define a prediction horizon, k, a positive integer denoting the number of frames to look before/after a tube to determine its potential connection. We consider each tube separately. When considering a tube, we check for other tubes that begin k frames after the end of (or that end k frames before the start of) the tube.

Consider finding a second tube to connect to tube **T**. First, we calculate an average Vx and Vy across the first (and last) frames of **T**. Using this velocity vector, we create a prediction ellipse where the entity would be k frames before the beginning and after the end of **T**. The prediction ellipse is compared with the beginning and end of the other tubes. We determine the tube that either begins (if the prediction ellipse is after **T**) or ends (if the prediction ellipse is before **T**) closest in space to the prediction ellipse and call this potential match **U**. If the prediction ellipse is within a spatial threshold (we chose 100 pixels) of **U** at the same frame *and* both tubes have similar velocity

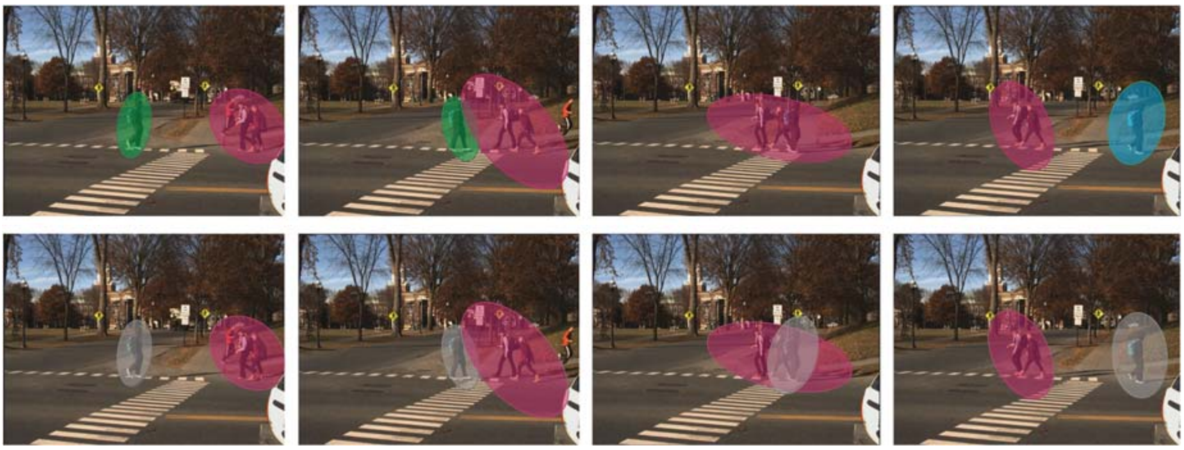

Figure 3: A scene before (top) and after (bottom) the implementation of Algorithm 4. The pedestrian with the backpack is occluded by the group of people walking oppositely. In the first video, the pedestrian's tube ends at the occlusion and a new tube begins once the group has passed. In the second video, we can keep track of the pedestrian even during the occlusion.

vectors (*Vx* and *Vy* signs match unless |V| <1), we combine the tubes into one. Otherwise, **T** remains unmatched. When two tubes are combined, the properties of the ellipses between the two tubes are interpolated.

We repeat this tube connecting process for all tubes. Furthermore, we conduct the process thrice, each at a different value of k (k = 5, k = 25, and k = 60). This connects tubes across occlusions up to two seconds long.

4 TOP DOWN STRATEGIES

Our localization framework offers the opportunity to insert feedback loops that use preliminary results to improve the quality of the tubes. We believe this is an advantage for scalability. In this section, we detail some of our feedback loops, which we denote as top-down methods. The methods discussed are not an exhaustive list, as we believe the possibilities for top down solutions are numerous.

Algorithm 4 (repeat at h=5, h=25, h=60)

Input: a list of tubes $\{\mathbf{T}_i\}_{i=1\ldots N}$, prediction horizon h
Output: a list of tubes $\{\mathbf{T}_i\}_{i=1\ldots K}$, $K \leq N$
For each tube $\mathbf{T}_i = \{e\}$
  Vx_F, Vy_F = average Vx, Vy of $[e_{n-4}, e_n] \in \mathbf{T}_i$
  Vx_B, Vy_B = average Vx, Vy of $[e_1, e_5] \in \mathbf{T}_i$
  e^*_F = using Vx_f, Vy_f predict ellipse at frame $max(e_f \in \mathbf{T}_i) + h$
  e^*_B = using Vx_b, Vy_b predict ellipse at frame $min(e_f \in \mathbf{T}_i) - h$
  G = {ellipse $g \in$ tube $\mathbf{U}_i$| $g_f \in [e^*_f - 5, e^*_f + 5]$}
  e' = closest $g \in$ G in distance to e^*
  If $|e^* - e'| < 100$ AND $\{e', e^*\}_{Vx,Vy}$ in same quadrant
    $\mathbf{T}_i = \mathbf{T}_i \cup \mathbf{U}_i$

Algorithm 4 connects tubes separated by several frames.

4.1 Magnocellular Sensitivity

As previously stated, the magnocellular-inspired low level image processing uses relative sensitivity to introduce an attention span based on size and motion. When a large, quickly moving object exits the frame, it creates a change in sensitivity. This effect increases the intensity value of the pixels in the magnocellular output as shown in Figure 4.

A false match created by a sensitivity effect is detrimental to the system's ability to keep track of an object. Rigid pairwise matching schemes experience difficulty with such outlier frames. Our sparse matching approach in Algorithm 2 is more robust to outlier frames.

In long periods with relatively small amounts of motion, the sensitivity effect can last for consecutive frames. To prevent the system from creating false matches as a result, we incorporate our knowledge about the tubes before and after the sensitivity effect.

We measure pixel intensities in each frame of the magnocellular output to detect the temporal borders of the prolonged sensitivity effect. Empirically, we expect a majority of pixels to be dark or mostly dark (intensity = 0–5). When the total number of non-dark pixels surpass the total number of dark pixels in a frame, we consider the frame a product of oversensitivity. Intermittent spikes of sensitivity are usually manageable because of our implementation of Algorithm 2, while prolonged areas of sensitivity can indicate a need for top-down solutions.

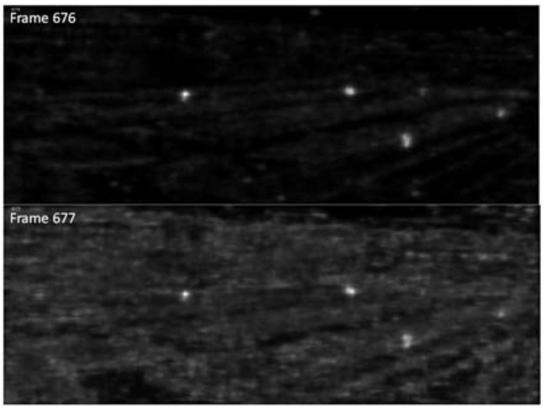

Figure 4: The visual result of a spike in magnocellular sensitivity. Analysis of this effect tells us when to consider top-down strategies.

We believe cases of prolonged sensitivity are regions that require feedback paths to repair trajectories in the region. In addition to measuring pixel intensities, we can also use our preliminary tube results to detect magnocellular sensitivity. For example, we consider the number of tubes present in each frame. The magnocellular sensitivity creates a large number of tubes that are short in duration. The sudden increase in the number of tubes corresponds to the area of sensitivity, as shown in Figure 5. Recognizing this phenomenon via the tube information from the first pass demonstrates our approach's unique propensity for incorporating feedback loops.

To remedy the effect of magnocellular sensitivity, we consider the tubes present immediately before and after the sensitivity effect. Using the velocity information from the former tube, we predict where we expect it to be after the effect. If a tube begins after the effect within a location threshold (we chose 100 pixels), we connect the tubes and interpolate the ellipse values between them.

4.2 Segmenting Object Tracks

An existing tube trajectory may need to be segmented for either of two reasons. The first is that the trajectory is corrupted with noise, in which case the spurious trajectory may be flagged. The second is that a tube trajectory may change to a different object; sometimes, multiple objects are caught in one tube track. Reasons for this may be that two objects became close to each other and were merged, or after one object stopped, a nearby object had similar motion characteristics and the initial tube construction therefore combined them. An example of this is shown in Figure 6. We can clearly see in a qualitative manner how the trajectory shifts from one object to another; fortunately, we can clearly see the difference in the trajectories as well.

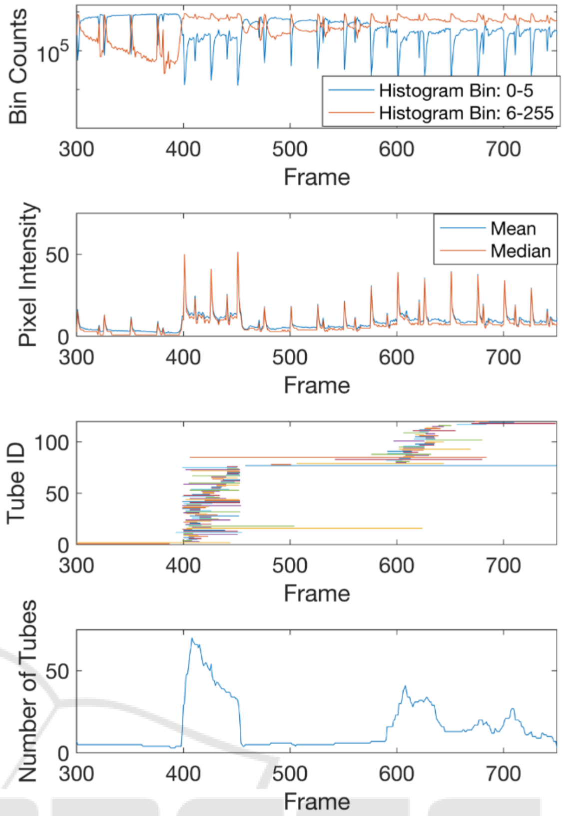

Figure 5: Histogram intensity counts of a magnocellular output (top). We consider magnocellular sensitivity when the orange line is above its blue counterpart. These same patterns are emulated in the mean and median pixel intensity lines (second). Tube identities and durations (third) are shown along with the number of tubes in each frame (last). Either of the above can be used to detect magnocellular sensitivity.

The correct subset of trajectories clusters well in space and time. Algorithm 5 identifies these clearly different trajectories and re-labels them as separate tubes. Algorithm 5 is a feedback process that does not necessarily have to be performed on every tube.

Algorithm 5 segments a given tube into smaller sections of consistent trajectories. After segmentation, the algorithm also recombines the sections. In this manner, noisy areas of the trajectory, or areas where the trajectory clearly shifted to another object are identified as separate tubes.

Algorithm 5

Input: a tube $\mathbf{T} = \{e^j\}_{j=1\ldots n}$
Output: a list of tubes $\{\mathbf{T}_k\}_{k=1\ldots K}$, $K \geq 1$
$\Gamma = \min[\text{median}(\{e_a\}), \text{median}(\{e_b\})]$
For each ellipse $\{e^j\} \in \mathbf{T}$
  $\Delta d_j = \text{EuclidianDistance}(\{e^j_{x,y,f}\}, \{e^{j+1}_{x,y,f}\})$
  If $\Delta d_j < \Gamma \rightarrow \mathbf{I}_j = \text{true}$
  Else $\rightarrow \mathbf{I}_j = \text{false}$
$\mathbf{S} = \{e^j \in \mathbf{T} \mid \mathrm{I}_j = 1\}$
$\{S_i\}_{i=1\ldots m} \subseteq \mathbf{S}$: groups of consecutive frames, e.g. $\mathbf{S} = \{e^1, e^2, e^5, e^6, e^7\}$
  $\rightarrow S_1 = \{e^1, e^2\}$, $S_2 = \{e^5, e^6, e^7\}$
For each $\{S_i\} \in \mathbf{S}$
  $x_0 = e^1_{x,y,f} \in S_i$, $x_1 = e^{end}_{x,y,f} \in S_i$
  $\overrightarrow{\alpha_i} = x_1 - x_0$, $\overrightarrow{\beta_i} = x_0 - x_1$
For each contiguous true section in $\mathbf{I} = \{S_i\}_{i=1\ldots m}$
  If Combine $(\alpha_i, \beta_{i+1}, \Gamma, S_i, S_{i+1}) \rightarrow$ Append S_{i+1} to $\mathbf{T}_k \mid S_i \in \mathbf{T}_k$
  Else $\rightarrow$ Define new tube, $\mathbf{T}_{k+1}$
    $S_i \in \mathbf{T}_k$
    $S_{i+1} \in \mathbf{T}_{k+1}$ | Make new tube

Function: Combine

Input: α_i, β_{i+1}, Γ, S_i, S_{i+1}
Output: Combine? True/False
If extension (α_i on $e^1 \in S_{i+1}$) $< \Gamma$ OR
  extension (β_{i+1} on $e^{end} \in S_i$) $< \Gamma$
  $\rightarrow$ Combine = true
Else $\rightarrow$ Combine = false

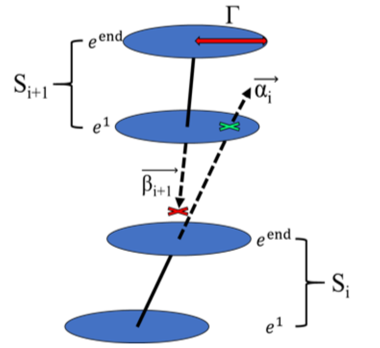

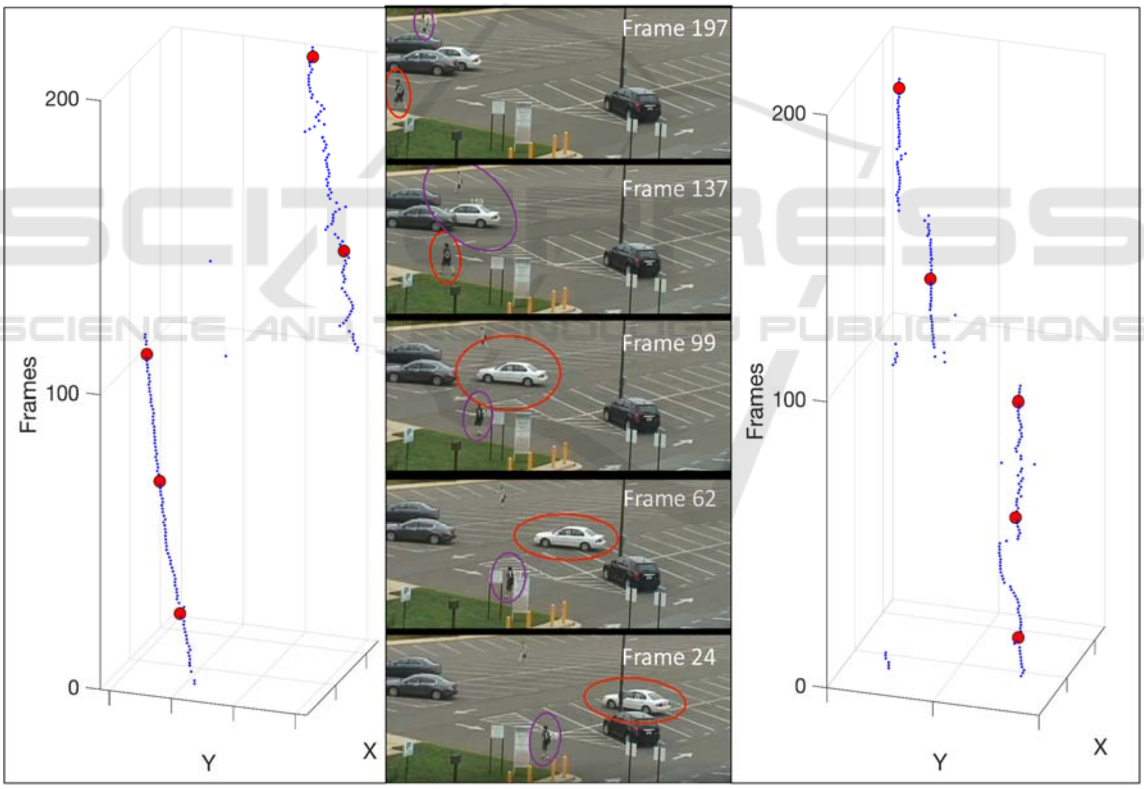

Figure 6: In the center, we see an example of tubes switching objects as they track. The red tube (left) follows the car as it moves across the parking lot, and then switches to the nearby pedestrian. Meanwhile, the purple tube (right) began on the pedestrian track and switched to the car, and then to another pedestrian. The dots in either trajectory correspond to the frames shown in the video (center).

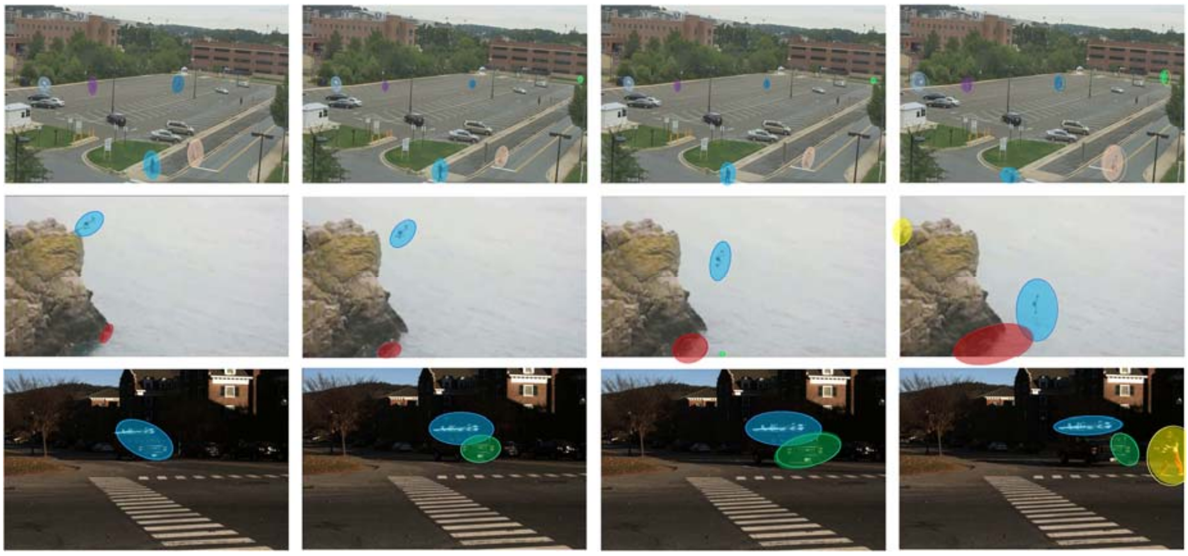

Figure 7: Three videos from separate datasets illustrating the results of our method. (Top) row is from the VIRAT video dataset, (middle) is from Thumos-15, and (bottom) is from our recorded dataset (Oh *et al.*, 2011; Gorban *et al.*, 2015; Ray and Miao, 2016) .

5 CONCLUSIONS

Action localization methods often require training data, supervision, and/or dense motion information. In this paper, we have presented a novel approach that performs unsupervised spatiotemporal action localization on videos in the wild without any of this information.

Our framework simultaneously localizes multiple actions and creates a compact macro representation of the associated spatiotemporal motion for each. Additionally, our approach does not require spatial information. Subsequent incorporation of spatial information within this framework offers exciting opportunity for improvement. For the above reasons, we believe our approach provides a strong foundation for object/action classification as well as broad possibility for top-down improvements.

ACKNOWLEDGEMENTS

We are grateful to Chris Kymn who contributed valuable ideas and approaches to this work. This work is supported in part by grants from the Office of Naval Research award number N00014-16-1-2359.

REFERENCES

Benoit, A., Caplier, A., Durette, B., & Hérault, J. (2010). Using human visual system modeling for bio-inspired low level image processing. Computer vision and Image understanding, 114(7), 758-773.

Brox, T., & Malik, J. (2011). Large displacement optical flow: descriptor matching in variational motion estimation. IEEE transactions on pattern analysis and machine intelligence, 33(3), 500-513.

Brox, T., & Malik, J. (2010, September). Object segmentation by long term analysis of point trajectories. In European conference on computer vision (pp. 282-295). Springer, Berlin, Heidelberg.

Caelles, S., Maninis, K. K., Pont-Tuset, J., Leal-Taixé, L., Cremers, D., & Van Gool, L. (2017). One-shot video object segmentation. In CVPR 2017. IEEE.

Chang, J., Wei, D., & Fisher, J. W. (2013). A video representation using temporal superpixels. In Proceedings of the IEEE Conference on Computer Vision and Pattern Recognition (pp. 2051-2058).

Fulkerson, B., Vedaldi, A., & Soatto, S. (2009, September). Class segmentation and object localization with superpixel neighborhoods. In Computer Vision, 2009 IEEE 12th International Conference on (pp. 670-677). IEEE.

Galasso, F., Shankar Nagaraja, N., Jimenez Cardenas, T., Brox, T., & Schiele, B. (2013). A unified video segmentation benchmark: Annotation, metrics and analysis. In Proceedings of the IEEE International Conference on Computer Vision (pp. 3527-3534).

Gavrila, D. M. (1999). The visual analysis of human movement: A survey. Computer vision and image understanding, 73(1), 82-98.

Giese, M. A., & Poggio, T. (2003). Cognitive neuroscience: neural mechanisms for the recognition of biological movements. Nature Reviews Neuroscience, 4(3), 179.

Gkioxari, G., & Malik, J. (2015). Finding action tubes. In Proceedings of the IEEE conference on computer vision and pattern recognition (pp. 759-768).

Gorban, A., Idrees, H., Jiang, Y. G., Zamir, A. R., Laptev, I., Shah, M., & Sukthankar, R. (2015). THUMOS challenge: Action recognition with a large number of classes.

Grundmann, M., Kwatra, V., Han, M., & Essa, I. (2010, June). Efficient hierarchical graph-based video segmentation. In Computer Vision and Pattern Recognition (CVPR), 2010 IEEE Conference on (pp. 2141-2148). IEEE.

He, K., Zhang, X., Ren, S., & Sun, J. (2016). Deep residual learning for image recognition. In Proceedings of the IEEE conference on computer vision and pattern recognition (pp. 770-778).

Horn, B. K., & Schunck, B. G. (1981). Determining optical flow. Artificial intelligence, 17(1-3), 185-203.

Jain, M., Van Gemert, J., Jégou, H., Bouthemy, P., & Snoek, C. G. (2014). Action localization with tubelets from motion. In Proceedings of the IEEE conference on computer vision and pattern recognition (pp. 740-747).

Jain, S. D., & Grauman, K. (2014, September). Supervoxel-consistent foreground propagation in video. In European Conference on Computer Vision (pp. 656-671). Springer, Cham.

Jiang, Y. G., Liu, J., Zamir, A. R., Toderici, G., Laptev, I., Shah, M., & Sukthankar, R. (2014). THUMOS challenge: Action recognition with a large number of classes.

Krizhevsky, A., Sutskever, I., & Hinton, G. E. (2012). Imagenet classification with deep convolutional neural networks. In Advances in neural information processing systems (pp. 1097-1105).

Kuehne, H., Jhuang, H., Stiefelhagen, R., & Serre, T. (2013). Hmdb51: A large video database for human motion recognition. In High Performance Computing in Science and Engineering '12 (pp. 571-582). Springer, Berlin, Heidelberg.

Lee, Y. J., Kim, J., & Grauman, K. (2011, November). Key-segments for video object segmentation. In Computer Vision (ICCV), 2011 IEEE International Conference on (pp. 1995-2002). IEEE.

Lu, Z. L., & Sperling, G. (1995). The functional architecture of human visual motion perception. Vision research, 35(19), 2697-2722.

Narayana, M., Hanson, A., & Learned-Miller, E. (2013). Coherent motion segmentation in moving camera videos using optical flow orientations. In Proceedings of the IEEE International Conference on Computer Vision (pp. 1577-1584).

Nguyen, A., Yosinski, J., & Clune, J. (2015). Deep neural networks are easily fooled: High confidence predictions for unrecognizable images. In Proceedings of the IEEE Conference on Computer Vision and Pattern Recognition (pp. 427-436).

Oh, S., Hoogs, A., Perera, A., Cuntoor, N., Chen, C. C., Lee, J. T., ... & Swears, E. (2011, June). A large-scale benchmark dataset for event recognition in surveillance video. In Computer vision and pattern recognition (CVPR), 2011 IEEE conference on (pp. 3153-3160). IEEE.

Oram, M. W., & Perrett, D. I. (1996). Integration of form and motion in the anterior superior temporal polysensory area (STPa) of the macaque monkey. Journal of neurophysiology, 76(1), 109-129.

Pathak, D., Girshick, R. B., Dollár, P., Darrell, T., & Hariharan, B. (2017, July). Learning Features by Watching Objects Move. In CVPR (Vol. 1, No. 2, p. 7).

Perazzi, F., Pont-Tuset, J., McWilliams, B., Van Gool, L., Gross, M., & Sorkine-Hornung, A. (2016). A benchmark dataset and evaluation methodology for video object segmentation. In Proceedings of the IEEE Conference on Computer Vision and Pattern Recognition (pp. 724-732).

Polana, R., & Nelson, R. (1994, November). Low level recognition of human motion (or how to get your man without finding his body parts). In Motion of Non-Rigid and Articulated Objects, 1994., Proceedings of the 1994 IEEE Workshop on(pp. 77-82). IEEE.

Poppe, R. (2010). A survey on vision-based human action recognition. Image and vision computing, 28(6), 976-990.

Ray, L., & Miao, T. (2016, June). Towards Real-Time Detection, Tracking and Classification of Natural Video. In Computer and Robot Vision (CRV), 2016 13th Conference on(pp. 236-241). IEEE.

Roth, S., Lempitsky, V., & Rother, C. (2009). Discrete-continuous optimization for optical flow estimation. In Statistical and Geometrical Approaches to Visual Motion Analysis (pp. 1-22). Springer, Berlin, Heidelberg.

Shi, J., & Malik, J. (2000). Normalized cuts and image segmentation. IEEE Transactions on pattern analysis and machine intelligence, 22(8), 888-905.

Shou, Z., Wang, D., & Chang, S. F. (2016). Temporal action localization in untrimmed videos via multi-stage cnns. In Proceedings of the IEEE Conference on Computer Vision and Pattern Recognition (pp. 1049-1058).

Simonyan, K., & Zisserman, A. (2014). Two-stream convolutional networks for action recognition in videos. In Advances in neural information processing systems (pp. 568-576).

Soomro, K., Zamir, A. R., & Shah, M. (2012). UCF101: A dataset of 101 human actions classes from videos in the wild. arXiv preprint arXiv:1212.0402.

Tokmakov, P., Schmid, C., & Alahari, K. (2017). Learning to Segment Moving Objects. arXiv preprint arXiv:1712.01127.

Tran, D., Bourdev, L., Fergus, R., Torresani, L., & Paluri, M. (2015). Learning spatiotemporal features with 3d convolutional networks. In Proceedings of the IEEE international conference on computer vision (pp. 4489-4497).

Tsai, D., Flagg, M., Nakazawa, A., & Rehg, J. M. (2012). Motion coherent tracking using multi-label MRF optimization. International journal of computer vision, 100(2), 190-202.
Tsai, Y. H., Yang, M. H., & Black, M. J. (2016). Video segmentation via object flow. In Proceedings of the IEEE Conference on Computer Vision and Pattern Recognition (pp. 3899-3908).
Wang, H., Kläser, A., Schmid, C., & Liu, C. L. (2011, June). Action recognition by dense trajectories. In Computer Vision and Pattern Recognition (CVPR), 2011 IEEE Conference on (pp. 3169-3176). IEEE.
Zhang, B., Wang, L., Wang, Z., Qiao, Y., & Wang, H. (2016). Real-time action recognition with enhanced motion vector CNNs. In Proceedings of the IEEE Conference on Computer Vision and Pattern Recognition (pp. 2718-2726).